UNIVERSITY OF CALIFORNIA
RIVERSIDE

Molecular Dynamics Study of Krypton Isotopes Physisorbed on Graphite

A Dissertation submitted in partial satisfaction
of the requirements for the degree of

Doctor of Philosophy

in

Physics

by

Karson D.W. Bader

June 2012

Dissertation Committee:
Dr. Allen Mills, Chairperson
Dr. Vivek Aji
Dr. Ward Beyermann

The Dissertation of Karson D. W. Bader is approved:

_____

_____

_____

Committee Chairperson

University of California, Riverside

Dedication

This would not have been possible without the help and encouragement from so many people: Kolin and Kegan Bader, Brad Hughes, Michael Roth, Julian Wilson, Paul Grey and Dan Angel. I want to express my deepest appreciation to: Dr. Allen Mills for his patience and understanding, Ron Sindric for putting me on the right path, and the most amazing person in my life, Melanie my wife, who has supported and encouraged me through every step.

To mom and dad: Thank you for shaping me into the person I am today.

ABSTRACT OF THE DISSERTATION

Molecular Dynamics Study of Isotope Separation via
Physisorbed Systems

by

Karson D. W. Bader

Doctor of Philosophy, Graduate Program in Physics
University of California, Riverside, June 2012
Dr. Allen Mills, Chairperson

We explore the difference in the rate of desorption of Krypton isotopes from a surface via Molecular Dynamics. Desorption of physisorbed Krypton isotopes is studied as a function of temperature and adsorbed layers. The model simulates a 50-50 mixture of Krypton isotopes where the multilayer systems are built around a first layer which is commensurate with the graphite substrate. It is shown that desorption of an isotropic mixture in a multilayered system (layers > 2) exhibits a separation that is equivalent to Graham's Law while a monolayer system exhibits a separation of the isotopes that is significantly higher. The enhanced effect seen in the monolayer studies may be due to the confinement provided by the graphite substrate. The validation was performed by calculating the vapor pressure of the system as well identifying the melting point of a commensurate monolayer of Kr physisorbed onto graphite. The limitations of the model as well as possible consequences are presented as well.

Table of Contents Page Number

List of Figures: Page Number

List of Tables: Page Number

Chapter 1 - Introduction to Isotope Separation

The field of isotope separation is an active area of research, defined as the process of concentrating desired isotopes of elements by removing other isotopes which may be comingled with them. The importance of isotope separation lies in its usage in both commercial and military applications, such as the development of nuclear fuel for both power stations and weapons.

In this chapter, I discuss the topic of isotope separation, which includes a brief description of the methods currently used, followed by the theoretical groundwork for adsorbed systems.

1.1: Isotope Separation

The origin of isotopes began with work that was done by Frederick Soddy[1] when he discovered that a radioactive element may have more than one atomic mass. This was immediately followed the discovery of isotopes of stable elements done by J.J. Thomson. Upon the discovery of neutrons, it was realized that isotopes of an element have the same number of protons and electrons, but different number of neutrons. The work done by J.J. Thomson is the first example of the technique to be known as mass spectrometry. It wasn't until 7 years later near the end of World War 1, the first mass spectrograph was built by Francis Ashton. Through the use of the mass spectrograph, Ashton was able to identify over 200 naturally occurring isotopes. While the discoveries of isotopes and

equipment to separate them, lead to significant advances in the areas of atomic and nuclear physics, the true push for the understanding of isotopes and methods to separate them came during the start World War II. Due to the realization that "extremely powerful bombs of a new type"[2] could be constructed by chain reaction in uranium, the scientific community, primarily due to the financial backing of the government, was able to make significant advances in both the understanding and practical usage of isotope separation. Due to these breakthroughs, the use of isotopes has become embedded in our daily lives. Medical imaging of radioactive isotopes allows patients to be diagnosed and treated by providing diagnostic information about a person's internal organs. In food preparation, radiation is used to prolong the shelf life of food before transportation. Even the smoke detectors located in almost every home in America contain a radioisotope, which assists in alerting the inhabitants of a possible fire. Through the continued research on isotopes and on methods to separate them, we have not only gained a better understanding of how the building blocks of nature works, but also have found numerous ways to enhance our everyday lives.

While there are several different techniques that have been created to separate isotopes, they fall into one of two categories; the separation is either dependent upon the mass difference of the isotopes or the differences in chemical reaction rates of the isotopes. Since volumes could be written on not only the history and the current level of research, as well as the dynamics behind the different methods of isotope separation; only the main

mechanisms of each method is introduced and the reader is directed to the included references if a deeper understanding is desired.

1.1a Diffusion

Regardless of the type of diffusion being discussed (thermal, atomic, surface etc.) diffusion is the process through which particles move from an area of higher concentration to an area of lower concentration. The equation for diffusion can be written as

$$\frac{\partial \phi(\mathbf{r},t)}{\partial t} = \nabla \cdot [D(\phi,\mathbf{r})\nabla \phi(\mathbf{r},t)]$$

where the density and the diffusion coefficient are given by $\phi(\mathbf{r},t)$ and $D(\phi,\mathbf{r})$ respectively. If the diffusion coefficient is assumed to be constant, then the diffusion equation becomes Fick's second law, which can describe how the concentration changes with time

$$\frac{\partial \phi(\mathbf{r},t)}{\partial t} = D\nabla^2 \phi(\mathbf{r},t)$$

The rate of movement of particles that are diffusing is dependent upon temperature and size of the particles. The difference has been approximated to the square root of the densities, otherwise known as Graham's Law[3]. For a mixture of two different isotopes:

$$\frac{Rate_1}{Rate_2} = \sqrt{\frac{\rho_2}{\rho_1}}$$

If the mixture is in thermal equilibrium, the two different isotopes will have the same energy but difference speeds:

$$\frac{1}{2}m_1v_1^2 = \frac{1}{2}m_2v_2^2$$

$$\rightarrow \frac{v_1}{v_2} = \sqrt{\frac{m_2}{m_1}}$$

Graham's law was the basis for the separating uranium during the Manhattan project during the 1940s. While isotope separation via diffusion has been done, current diffusion plants are slowly being removed from production and are being replaced with gas centrifuge technology.

1.1b Centrifuge Method

The first successful separation of isotopes using the centrifuge method was done with chlorine in 1936[4].The system is designed around having gas fed into a cylinder that is then rotated at high speeds. The heavier gas will migrate towards the outer edges of the cylinder while the lighter components of the gas will collect near an inner cylinder at the center due to the centrifugal force on the isotope. The lighter components are collected and then fed into another cylinder repeating the processed until the desired purity is achieved. Since the initial design, several advancements have been made that have used the centrifugal effect scheme. The exact details of current isotope separators using this method is a closely guarded secret considering it is one of the cheaper and easier methods available to separate Uranium for either nuclear reactors or nuclear weapons.

1.1c Electromagnetic Method

Similar to mass spectroscopy, the electromagnetic method of isotope separation uses charged isotopes that are deflected by a magnetic field. The amount of deflection of each isotope depends on the isotopes mass. This basic design, separation via charged isotopes and looking at their deflection is the idea behind mass spectroscopy. While a mass spectrometer is primarily used for determining the composition of a gas, a mass spectrometer that has been modified to collect isotopes is known as a calutron. The charged particles travel into a chamber where a magnetic field that is perpendicular to their velocity provides a centripetal force on the isotopes.

$$\frac{mv^2}{r} = q\vec{v} \times \vec{B} = qvB$$

since the ions of the different isotopes have the same charge, the lighter isotopes will be bent more in the magnetic field.

$$r = \frac{mv^2}{qvB}$$

While the design behind a calutron is easier to reproduce compared to the other isotope separation methods, it is not able to achieve an output that is comparable to other well known methods. Because of the small output achieved through the use of a calutron it is predominately useful for producing small amounts of isotopes at higher levels of purity, but it is impractical to use for the production of large amounts.

Besides the methods previously listed there are a handful of other methods that have been used for isotope separation: atomic vapor laser isotope separation, molecular laser isotope separation, or even separation based on chemical reaction rates. These methods are either

early in the development stage or not relevant to the discussion on Krypton isotopes, so they will not be discussed in this dissertation.

1.2 Theory adsorbed systems

The research to be presented involves Krypton isotopes physisorbed onto a graphite surface; therefore the theory and mechanisms of adsorption/desorption needs to be discussed. This is followed by a short discussion on the importance of multi-layer effects on adsorbed systems, or more importantly, desorbing systems.

Adsorption is defined as the adhesion of atoms, molecules etc. to a surface. The mechanism of adsorption is a result of the interaction between the adsorbate and the adsorbent. While the exact detail is dependent upon the species, physisorption (physical adsorption), is generally characterized as an interaction of Van der Waals forces. The opposite of adsorption, is desorption which is defined as a substance being released from or through a surface. The rate of desorption, R, of an adsorbate from a surface can be expressed by the following:

$$R = kN^x$$

Where k is the rate constant and N is the surface concentration of the species that is adsorbed. The order of desorption, x, can usually be predicted depending on the type of desorption[5] where:

Atomic Desorption

$$Kr_{(adsorbed)} \rightarrow Kr_{(gas)}$$

would be considered a first order process, x = 1 and,

Recombinative Desorption

$$2\,O_{(adsorbed)} = O_{2(gas)}$$

would be considered a second order process, x = 2.

The rate constant k can be expressed in an Arrhenius form[6]

$$k = Ae^{-E_a/k_bT}$$

Which allows the desorption rate to be to be expressed as a function of temperature.

$$R = AN^1e^{-E_a/k_bT}$$

The equation given above is known as the Polanyi-Wigner equation for the rate of first order desorption. The variable A, known as the pre-exponential factor describes the attempt frequency of the atom/molecule to overcome the barrier to desorption[7], k_b is the Boltzmann constant and $e^{-E_a/RT}$ gives the fraction of atoms which have an energy equal to or greater than the activation energy. It is generally assumed that both the attempt frequency and the desorption energy are dependent on temperature and coverage[8].

The more recent theories used to describe adsorption and desorption are based on the lattice gas model. The surface of the solid is divided into two-dimensional cells, usually labeled i, where one introduces another variable $n_i = 0$ or 1, depending on whether the cell is occupied or not by an adsorbed atom. In a model presented by Payne and Kreuzer[9], they investigated adsorption and desorption based on a lattice gas with nearest neighbor

and next nearest neighbor interactions in and between layers. With the model they proposed they were able to reproduce many of the equilibrium properties that have been seen in related experiments through the use of transfer matrix techniques. While the model used in their investigation was in close agreement with relevant experimental data, there were a few flaws. The most notable limitation imposed in their model was that on-top growth for the additional allayers in the system was used. In multi-layer growth it is assumed that additional atoms placed onto complete layers would sit in, but shifted in the positive z direction, hollow sites with respect to the atoms beneath it. In the model proposed by Payne and Kreuzer, they suggested that using on-top growth would serve to enhance confinement of the atoms beneath it. To prevent the enhanced confinement seen in an on-top multi-layer model, the model we designed, described in chapter 2, has each layer initially placed such that all the atoms fall within the hollow sites of the atoms beneath it.

Another multilayer model, derived by Asada and Sekito[10] used a similar lattice gas model as Payne and Kreuzer except their multilayer system was one of restricted atom stacking. This design requires that when an atom is placed in an upper layer, it must be in contact with at least x ($0 < x \leq m_1$) underlying atoms. Where x is referred to as the atomic stacking condition and m_1 is the number of sites in a neighboring layer. With the desorption rate defined as the sum of the rates of individual first-order kinetic process, they discovered that when the lattice gas system is in the two phase coexistence regime, desorption is found to follow zero-order or quasi zero-order kinetics.

Chapter 2: Computational Method

To make the following sections easier to understand, the whole simulation will be briefly described here. This will allow one to see how each of the pieces described below factors into the simulation as a whole.

The model used is a constant temperature molecular dynamics simulation consisting of a binary mixture of krypton atoms of different mass and various layers adsorbed onto a graphite sheet. The interactions between the krypton and graphite surface are modeled through the use of an interaction potential while the Kr-Kr interactions are modeled through a standard Lennard Jones potential. The isotopes are equilibrated at 50 Kelvin for 100 ps before being run at T=110-130 Kelvin until half of the isotopes have desorbed from the system. The position, velocity, and acceleration of each particle are updated via the velocity Verlet algorithm and the temperature of the system is kept constant through the means of velocity rescaling. When the isotopes reach a position that is 3σ above the initial placement of the highest layer of isotopes, they are considered to have desorbed from the system and those isotopes are not included in the velocity rescaling to prevent the effect of cooling on the system below or in the force calculations.

The first section describes the potentials used to model the interaction between the Krypton and graphite surface and the Kr-Kr atoms. This is followed by a discussion on

the choice of initial placement for the Krypton atoms with respect to the graphite surface as well as the placement of each layer of Krypton that is placed with respect to the layer beneath. The third section covers method of temperature control used in this simulation as well as the effects of surface cooling when a particle leaves from a surface. Following is a section that will describe the techniques used to calculate the equations of motion for each isotope in the system. Since there are numerous integrators available (Verlet, velocity Verlet, gear-predictor, etc.) as well as different short and long range interaction algorithms (Verlet lists, Ewald summation, Particle Mesh Ewald, etc.) only the algorithms used to conduct the research will be derived and discussed. If the reader wishes to know more information on the advantages and disadvantages of other available algorithms, the references are provided[11].

Section five discusses the methods available to choose the proper time step in a Molecular Dynamics simulation. Section six covers the topic of how desorption is determined in the simulation and finally, section seven covers the topic of validating the molecular dynamics simulation.

Section 2.1 Potential and Boundary Conditions

At the core of any Molecular Dynamics program is the calculation of the potential energy within the system. Through the potential the forces acting on each atom or molecule can be calculated and thus its position and velocity updated after each timestep. Not only is

the choice of the potential one of the largest and most important components of a MD simulation, it is also the most expensive computationally. If there were a total of N atoms in a simulation it would require a total of $N^2 - N$ calculations to calculate pair interactions between each of the atoms. To reduce the amount of time it would take to perform $N^2 - N$ calculations, boundary conditions are implemented to facilitate faster computation cycles with little lose to accuracy. Following is the details of the potential that is used as well as the boundary conditions that were implemented in our model.

2.1a Steele potential:

When dealing with Krypton atoms physisorbed onto graphite, there are two ways to calculate the interaction. The first and the most accurate would be to place Carbon atoms in a hexagonal lattice[12] and to calculate the interaction of each Carbon atom with not only each other, but with each Krypton atom as well. While this would be the most accurate, it would also be computationally expensive since the longest part of any simulation is the calculation of the forces. An easier method would be to use an interaction potential that would take into account the affects of all the carbon atoms thereby saving computation time. The potential interaction used in our research between the Krypton atoms and the graphite is of the form proposed by Steele [13]

The potential of the graphite is of the form:

$$u_i^{gr} = E_{oi}(z_i) + \sum_{n=1}^{\infty} E_{ni}(z_i) f_{ni}(x_i, y_i)$$

The first term is known as the holding potential which is the stronger of the two terms that provides the attraction or repulsion between the graphite and the other atoms in the system. The second term, known as the corrugation potential, provides the lateral forces that are present in the system as the adsorbate travels across the graphite surface.

The holding potential is derived by considering the interaction between a single carbon atom and adsorbate atoms. Representing this interaction as a Lennard-Jones pair potential:

$$u(r) = 4\varepsilon[\frac{\sigma^{12}}{r^{12}} - \frac{\sigma^{6}}{r^{6}}]$$

Now consider a continuous mass distribution (representing each graphene plane, made of up of n total planes with plane indices p), where the distance between the two atoms is represented as

$$r = \sqrt{x^2 + y^2 + z^2}$$

This can be rewritten as:

$$r^2 = (z + pd)^2 + \rho^2$$

Now the Lennard Jones equation can be rewritten as:

$$u(r) = 4\varepsilon\sigma^6[\frac{\sigma^6}{((z+pd)^2+\rho^2)^6} - \frac{1}{((z+pd)^2+\rho^2)^3}]$$

Now expressing $E_o(z)$ as an integral over an infinite graphene sheet and writing the differential term in terms of the in-plane radius ρ and ϕ.

$$E_o(z) = \int u(z,\rho,d)\sigma\rho \; d\rho \; d\phi$$

Where σ, defines the number density is the number of carbon atoms per graphite unit cell over the surface area of a single graphite cell. The final form of the holding potential can finally be written as:

$$E_o(z) = 4\varepsilon\sigma^6(\frac{q}{a_s})\int_0^{2\pi}\int_0^{\infty}[\frac{\sigma^6}{((z+\_pd)^2+\rho^2)^6} - \frac{1}{((z+\_pd)^2+\rho^2)^3}]\rho \; d\rho \; d\phi$$

due to the azimuthal symmetry in each graphite plane and summing over an infinite number of graphene indices, the final form of the holding potential can be written as

$$E_o(z) = \frac{2\pi\varepsilon q\sigma^6}{a_s}(\frac{2\sigma^6}{45d(z_i+0.72d)^6} + \frac{2\sigma^6}{5z_i^{10}} - \frac{1}{z_i^4} - \frac{2z_i^2+7z_id+7d^2}{6d(z_i+d)^5})$$

Solving for the second term in the Steele expansion is done in a similar fashion:

$$E_n(z) = \frac{2\pi\varepsilon\sigma^6}{a_s}(\frac{\sigma^6}{30})(\frac{g_n}{2z_i})^5 K_5(g_nz_i) - 2(\frac{g_n}{2z_i})^2 K_2(g_nz_i)$$

And

$$f_1(x_i, y_i) = f_n(x_i, y_i)$$

$$f_n(x_i, y_i) = -2[\cos(\frac{2\pi}{a}(x + \frac{y}{\sqrt{3}})) + \cos(\frac{2\pi}{a}(x - \frac{y}{\sqrt{3}})) + \cos(\frac{4\pi}{a}(\frac{y}{\sqrt{3}}))]$$

Since the sum quickly converges in the equation above, only the first term is kept.

The most straight forward test of a given model for the gas-solid interaction energy is based on a comparison between experimental Henry's constants and theoretical gas-solid virial coefficients[14 15]. The formula derived by Steele has been determined to be one of the simplest methods that can be used to model the interaction between an adsorbate and an adsorbent and one that is soundly based on the statistical mechanical description of physisorption behavior that has been well studied over the past 40 years[16].

2.1b Lennard Jones Potential:

A key step to any molecular dynamics simulation is the calculation of the acceleration of the particles involved. The collisions between particles in a simulation are due to the forces that act on each particle. To determine the forces on each particle requires knowing the interaction potential between each of the particles. For the investigation of isotope separation in an adsorbed system the standard 12-6 Lennard Jones potential is used:

$$u_{LJ}(r_{ij}) = 4\varepsilon[(\frac{\sigma}{r_{ij}})^{12} - (\frac{\sigma}{r_{ij}})^{6}]$$

The Lennard Jones potential is comprised of two pieces, one representing long range interactions and the other representing short range interactions. The r^{-6} term represents the Van der Waals force which is the weak attraction felt from the electric dipole moments between atoms. While the r^{-12} term represents the strong repulsive force that results from the overlap of the electron clouds, otherwise describing Pauli repulsion. The advantage of using the Lennard Jones potential is threefold; 1) it is a continuous potential that can be easily used , 2) it is can easily handle volume fluctuations that may be involved in some simulations, 3) requires less computation compared to other potential interaction models. It is well known that the 12-6 LJ potential is not a 100% faithful representation of the potential interaction between particles[17], and that there are several other models that are available that give a more accurate representation such as the Stockmayer potential and the full configuration interaction to name a few. The disadvantage to the numerous other methods for calculating the potential interaction lies in their expensive computation time, thereby not only limiting the number of atoms that can be used but the number of simulations that can be run due to available resources. For these reasons and considering the vast body of research that has used Lennard Jones potentials for comparison, as well as the how long the simulations need to run to gather useful date; the Lennard Jones potential was determined to be the best candidate to model the inter-atomic potential.

2.1c Boundary Conditions:

Since the aim of Molecular Dynamics is provide useful information about physical systems, the size of the system simulated is limited by both hardware speed and availability. This being the case, MD is still able to accurately simulate real world experiments with the use of proper choice of periodic boundary conditions. Periodic boundary conditions are used to create the illusion that there is an infinite system of identical copies surrounding the region of interest, thereby removing edge effects. During the simulation as an atom moves around it has a periodic image that mimics every single movement in each of the neighboring boxes as in Fig. 2.1a

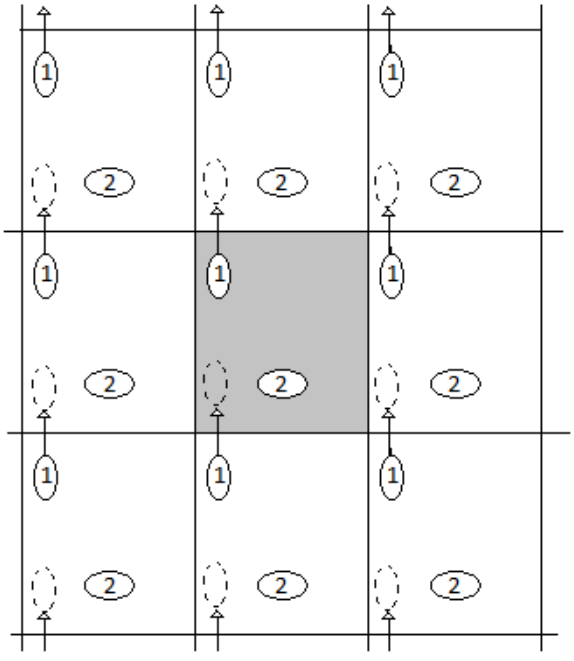

Fig. 2.1: A two-dimensional representation of a periodic system. The box in the center is the computational cell being modeled. As an atom or molecule moves around the computational cell its image would mirrored in the surrounding cells. If the particle happens to cross over a boundary, its image would enter through the other side creating the illusion of an infinite system.

The advantage of using periodic boundary conditions is that each particles image does not need to be stored. When a particle crossed over a boundary its position is either added or subtracted by the length of the box to bring it back into the main computation area, assuming 2D periodic boundary conditions. While the periodic boundary conditions remove the edge effects in a simulation, the complication of the sheer number of calculations that need to be performed still needs to be addressed as well as prevent a particle from seeing its' image when calculating the forces.

Preventing a particle from calculating the force on itself is done through what is known as the minimum-image convention[18]. The minimum-image convention is a method which each particle interacts with the closest image of the other N-1 particles. By using the minimum image convention, the calculation due to pairwise-additive interactions is reduced to $\frac{1}{2}(N^2 - N)$ from $N^2 - N$. In an effort to further speed up calculations and/or use larger systems, a cutoff distance can be used when calculating the potential interaction from nearest neighbors. If r is the distance between two particles and the cutoff distance is r_c, when $r \geq r_c$, the potential interaction is set to zero. If the simulation is a box of side L, then the number of neighbors considered is reduced by a factor of $4\pi r_c^3 / 3L^3$, thereby granting a huge savings in time. While implementing a cutoff radius reduces computation time, two important guidelines needs to be followed:

1) The value of the cutoff should be large enough to prevent any large perturbations within the system. In our simulation of Lennard Jones atoms a cutoff radius of $r_c = 4\sigma$ is used. With a cutoff of 4σ the value of the pair potential is 0.098 percent of the well depth. While the choice of 4σ for the cutoff distance is almost twice the standard value recommended for most MD simulations of LJ particles, it permits more accurate results but requires a longer computation time.

2) The cutoff distance must not be greater than ½ L. This is to be consistent with the minimum-image method by preventing the particles from seeing their image when calculating the pair potentials.

2.2 Isotope Placement

The effects of placement and density of rare gases adsorbed onto graphite has been extensively studied and is well documented[19 20 21] and ref 1-19 within ref (16). Even though the investigations involve rare gases, they provide a wealth of information, ranging from melting transition, adsorption isotherms and even pure and mixed diffusion coefficients. This is especially true in the case of Krypton adsorbed onto graphite where numerous studies have been done experimentally, theoretically and computationally[22 23 24 25 26].

Previous studies have shown that Krypton monolayers adsorbed on graphite surfaces exhibit a $\sqrt{3}$ x $\sqrt{3}$ R 30^o structure that is commensurate with the graphite basal plane [27 28], see Fig 2.2.

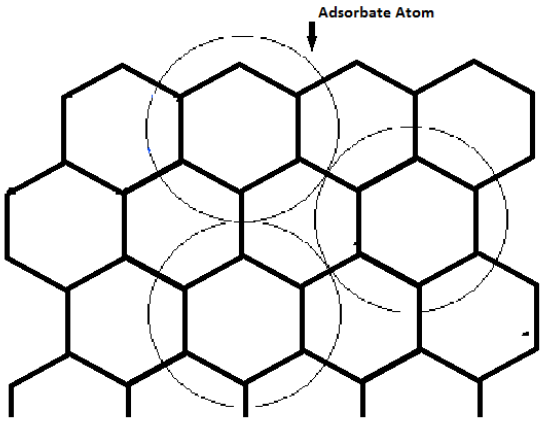

Fig. 2.2 Registered $(\sqrt{3}$ x $\sqrt{3})$ structure of monolayer of Krypton on graphite

To design a system with multiple layers, every even layer is shifted 1.8Å along the x and y axis and 3.6 Å above the Krypton layer below, while every odd row is placed in the same configuration with the first row in agreement with the parameter values listed in Table 1 on page 35. By placing the isotopes in this structure, we are attempting to reduce the amount of time needed for the system to reach equilibrium. To prevent any type of biased configuration, the masses are assigned randomly for every simulation as well as the initial velocities. The system is then allowed to equilibrate for 100ps at $T_o = 50$ Kelvin so any initial memory of the system's initial setup is removed.

2.3 Temperature Scaling

Besides the choice of the potential, the next decision important decision is how handle the temperature control in a molecular dynamics simulation. The most straightforward method to control the temperature is known as velocity rescaling. The derivation for the velocity rescaling term originates from the Maxwell-Boltzmann distribution and determining the average the average kinetic energy. The average kinetic energy is defined as:

$$< K >=< \frac{1}{2} mv^2 >= \int_0^\infty \frac{1}{2} mv^2 f(v) dv$$

f(v) can be found from the Maxwell-Boltzmann distribution of speeds

$$f(v) = 4\pi (\frac{m}{2\pi k_b T})^{\frac{3}{2}} v^2 e^{-\frac{mv^2}{2k_b T}}$$

Substituting f(v) into the equation for the average kinetic energy

$$< K >= 2\pi m (\frac{m}{2\pi k_b T})^{\frac{3}{2}} \int_0^\infty v^4 e^{-\frac{mv^2}{2k_b T}} dv$$

It can be seen that the above integral has the form

$$\int_0^\infty x^{2s} e^{-ax^2} = \frac{(2s-1)!!}{2^{2+1} a^s} (\frac{\pi}{a})^{\frac{1}{2}}$$

Let x=v , s=2 and a= m/2kT

$$< K >= (2\pi m(\frac{m}{2\pi k_b T})^{\frac{3}{2}}) \frac{3!!}{8(m/2kT)^2} (\frac{2\pi kT}{m})^{\frac{1}{2}}$$

Therefore,

$$< K >= \frac{3}{2} k_b T$$

In a system of N particles, the relationship between the average kinetic energy and the instantaneous temperature is

$$\frac{1}{2}\sum_i m_i v_i^2 = \frac{3}{2} N k_b T'$$

Therefore to keep the temperature T' = T_o, all the velocities in the simulation can be rescaled to a new velocity by

$$v'_{i,\alpha} = \sqrt{\frac{T_o}{T'}} v_{i,\alpha}$$

In the simulation used to investigate isotope separation in an adsorbed system, the system temperature is checked, and scaled if necessary, once per step cycle and only involves the isotopes that have not yet desorbed.

2.4 Choice of Integrator

The basic structure of any Molecular Dynamics program is, given the position, velocity etc, at a time t, determine the position, velocity, etc at some time t + δt within some degree of accuracy. The choice of δt is such that it is significantly smaller than the typical

time taken for a molecule to travel its own length[11]. While there are several algorithms that have been developed that fall into the basic structure previously described, only the integrator used in our work will be reviewed. Coverage of the advantages, disadvantages and comparison to the other algorithms is well documented[11]; therefore they will not be discussed here.

2.4a Velocity Verlet Algorithm

Since Molecular Dynamics is used to study the behavior of particles over time, Newton's laws must be solved. Since Newton's laws are ordinary differential equations, the finite difference method is used to solve or 'predict' the next positions. This is done by taking the Taylor expansion of the position, velocity and acceleration about t:

$$r(t+\delta t) = r_o(t) + \delta t v(t) + \frac{1}{2}\delta t^2 a(t) + \ldots$$
$$v(t+\delta t) = v_o(t) + \delta t a(t) + \ldots$$
$$a(t+\delta t) = a(t) + \ldots$$

Starting with the initial position, velocity and acceleration of each particle, each term is updated at a time $t+\delta t$ later , where δt is chosen such that it is much smaller than: a) the time it would take for an atom to travel its own length or b)the fastest vibrational frequency in the system. By using the information above, different integration methods can be derived to calculate a particle's new position or velocity.

The most common of the integrators is called the velocity Verlet integrator. The algorithm is implemented by updating the position and then the velocity after calculating the new acceleration:

$$\vec{x}(t+\delta t) = \vec{x}(t) + \vec{v}(t)\delta t + \frac{1}{2}\vec{a}(t)\delta t^2$$
$$\vec{v}(t+\delta t) = \vec{v}(t) + \frac{1}{2}(\vec{a}(t) + \vec{a}(t)\delta t)\delta t$$

Two points need to be made about the above algorithm: 1) The updated acceleration is $\vec{a}(t+\delta t)$ derived from the potential at the updated position $\vec{x}(t+\delta t)$, 2) The Velocity Verlet algorithm also assumes that acceleration is independent of the velocity.
In using the above method, two sources of error show up; the first is the round off error that occurs due to computational rounding, the second is due to the truncation of the Taylor expansion. The error in the position and velocity is due to the Taylor expansion in derivation of the velocity Verlet algorithm[29]:

$$x(t+h) \approx x(t) + hv(t) + \frac{h^2}{2} f(x(t)) + O(h^3)$$
$$v(t+h) \approx v(t) + hf(x(t)) + \frac{h^2}{2} v''(t) + O(h^3)$$

Now, to solve simplify the velocity term, do a Taylor expansion about t+h but in the opposite directions:

$$v(t+h-h) \approx v(t+h) - hf\,(x(t+h)) + \frac{h^2}{2} v''(t+h) + O(h^3)$$

Solving for $v(t+h)$

$$v(t+h) = v(t) + hv'(t+h) - \frac{h^2}{2} v''(t+h) + O(h^3)$$

Averaging both expressions for $v(t+h)$:

$$v(t+h) = v(t) + \frac{h^2}{2}(v'(t) + v'(t+h)) + \frac{h^2}{4}(v''(t) - v''(t+h)) + O(h^3)$$

By applying the mean value theorem and assuming that f" is bounded, the h^2 term can be eliminated resulting in the final form of the velocity:

$$v(t+h) = v(t) + \frac{h}{2}(v''(t) + v''(t+h)) + O(h^3)$$

The last term in the positions and velocity signify the local error due to truncation. Since the local error is due to one iteration, the global error is defined as the error at the final time $t_o + t$. If the local truncation error is h^{k+1} the global error is usually one order higher, h^k, due to the accumulation of error with the integration steps[30].

2.5 Choice of Timestep in Molecular Dynamics Simulations

Since the processes of updating the positions are an iterative one, the proper step size must be chosen to ensure CPU time is not wasted if Δt is too small or error is introduced if Δt is too large. The importance of the proper time step can be understood by looking at the position of a ball as it is thrown at a wall. When updating the position as the ball nears the wall, if the time step is really large, the new position could have the location of the ball placed inside the wall. If the ball approaches the wall and the time step is extremely small it would take several iterations of calculating the position until the ball reaches a point where it would actually collide with the wall. This would result in a program that is not efficient due to excessively long calculation times[31].

Another method employed to confirm that the timestep was chosen properly was to graph the kinetic energy of the particles vs. time as well as looking at the temperature of the system vs. time. When the time step is large, one of the ways that error is introduced is by allowing the atoms to get closer to one another than they should be. This causes the forces felt on each atom to be larger, which in turn increases the kinetic energy of that atom before the next iteration. If left unchecked long enough, the kinetic energy of the system will keep increasing until either the program crashes or the program finishes with the date being unreliable.

Another possible method to get an approximation of what timestep should be used is to follow the method proposed by Choe and Kim[32]. They investigated how it could be

possible to determine the proper timestep by analysis of the eigenvalues to explain the relationship between the timestep and the dynamics of the system. While the method proposed by Choe and Kim, used a simple harmonic potential for the interaction energy in a hydrogen molecule to calculate the eigenvalues, the method would be extremely difficult for more complex potential such as the Lennard Jones potential.

The last method that could be used to determine the appropriate time step would be to perform several short simulations, each with a different time step and each starting from the same initial configuration. Once the simulations have run for the same total time, the Verlet algorithm should give RMS energy fluctuations which are proportional to δt^2 [33]. A good initial guess of δt^2 is that it should be an order of magnitude smaller than the fastest vibrations being modeled in the system[11].

What should be mentioned is that the choice of time step is still purely a mechanical issue. It deals with the correct solution to Newton's laws and does not allow any statements to be said about whether thermodynamic equilibrium has been reached. This can only be said by comparing the simulation results to well known thermodynamic properties, which will be discussed in the upcoming sections.

2.6 Desorption Limit

One of the main components of this work was centered on capturing the rate at which isotopes actually evaporate from the system. Several studies have calculated the diffusion coefficients based on mass dependence and the self diffusion coefficients of Kr[34]. While

the previous research calculated the diffusion coefficients based on either Einstein's mean-square displacement or by integration of the velocity autocorrelation function using the Green-Kubo relation, nothing has been done to analyze the evaporation rate via the trajectory of each of the individual particles. To calculate when a particle has desorbed from a system a distance above the Kr-graphite system needs to be specified. The distance selected is based on the Lennard Jones potential being used in the simulation. By selecting a distance that is 3σ above the highest layer of Krypton after equilibrium, the interatomic potential is 1/180 or 0.545% of the potential well depth. When a particle reaches a vertical distance (perpendicular to the graphite sheet) that is 3σ above the equilibrium position of the highest Krypton layer, it is removed from the system. The particles are removed from the system by being removed from the force calculations as well as the kinetic energy calculations to prevent cooling of the Kr-graphite system. Besides being removed from the force calculations and the calculation of the system temperature, the particles are also physically removed from the environment to prevent the possibility of having desorbing isotopes interacting with 'ghost' isotopes.

2.7 Validation of Molecular Dynamics Simulation

One of the most important steps in doing research that involves computer simulations is ensuring that the program is giving valid results. Validation is especially important if the results show something new and/or unexpected. If the results are new or unexpected, one or both of the following has occurred[35]:

I. A new phenomenon has been found.

II. The results are wrong, because

1. the model that was used is inappropriate for the application,
2. the force field is inadequate ,
3. the results have not converged due to insufficient sampling,
4. the software contains bugs,
5. the software has been used incorrectly.

To ensure the program is valid, each of the above points will be addressed individually along with the appropriate graphs and/or data.

2.7a Choice of Model

This research is based on looking at the desorption rate of adsorbed isotopes. To this end, any model created needs to involve the following:

a) Atoms of different masses

b) Appropriate interaction potential between both the atoms and the substrate

c) Accurate method of keeping track of each particles position and velocity

d) Method of determining when particles have desorbed from the system

Addressing each of these point by point:

a) In the simulation the system is made up of a 50% mixture of each of the two masses. To prevent bias, the atoms are commensurate with the graphite and the masses are randomly assigned at the start of the simulation. Once the masses have been randomly assigned, the initial velocities are randomly assigned according to the Maxwell-Boltzmann distribution at the temperature of interest.

b) The choice of the interaction potential is based off of previous research that has investigated the diffusion coefficient in either pure or mixed systems using similar interaction potentials and algorithms. By using similar potentials our results can be compared to the vast collection of research based on these systems[16 36 37].

c) The accuracy and effectiveness of using the velocity Verlet algorithm is well documented and is considered one of the standard algorithms to use in Molecular Dynamics[11]; therefore the ability of keeping track of the particles is not in question.

d) Since the point that a particle evaporates is highly dependent upon the potential used, the decision to use 3σ is based on the standard cutoff radius ($r_c=2.5\sigma$) that is used by the majority of LJ simulations[11].

2.7b Choice of potential and corresponding parameters

There are 3 distinct properties when talking about molecular systems; 1) Structural, 2) Energetic, and 3)Dynamical properties. Each property has several components that could be tested and compared to experimental or theoretical result. To validate our use of the LJ interatomic potential and the Steele potential, the heat of vaporization was calculated, as well as the melting and boiling points of Krypton.

By comparing our simulated results with the values calculated experimentally and theoretically for Krypton monolayer physisorbed onto graphite, we are able to determine whether the potential and parameters were chosen wisely. The comparison of our data with the expected values can be found in the section discussing software quality.

2.7c. Equilibration time > Relaxation time for measured property

In molecular dynamics the program is usually broke up into two pieces: the equilibration phase and the production phase. The equilibration phase is necessary for two reasons, the first is that no matter how carefully you design the system or set the initial parameters, the system won't be in its most 'relaxed' state. The second reason the equilibration phase is needed is because it prevents any type of bias that may be introduced into the system by the user.

To prevent bias and to make sure the system starts out in a stable state, the instantaneous potential energy and/or pressure should be recorded. The equilibration period should be

extended at least until these quantities have ceased to show a systematic drift and have started to oscillate about steady mean values[11].

2.7d. Software Quality

While there are a handful of definitions that could be used to define software quality, what is going to be addressed are the reliability and efficiency of the program that was created (The topics of security, maintainability and size when talking about the quality are going to be ignored). The only way the reliability of the program can be addressed is by using the program to calculate parameters or values that can be compared to theoretically and experimentally accepted data.

To satisfy this requirement, both the melting temperature of a monolayer of krypton on graphite and the vapor pressure of a multi-layer krypton system adsorbed onto graphite were measured.

To measure the vapor pressure, 5 layers of krypton, 100 atoms per layer, were adsorbed onto graphite. The system is allowed to equilibrate for 100 ps at 50 K before being at ran at 5 different temperatures till 20% of the particles have left the system. The desorption rates are converted to an effective vapor pressure, $P_{vap} = R_d(4RT / \bar{v}\ \bar{s})$, where R is the gas constant, v is the mean molecular speed and s is the average sticking coefficient. The vapor pressure is extrapolated back to t = 0 and fitted to the vapor pressure curve given by the Clausius-Clapeyron equation, $P_{vap} = P_0 \exp\{-\lambda_{vap} / RT\}$, Fig. 2.3. The calculated heat of vaporization is λ_{vap} = (10.6±0.5)kJ mole^{-1} which is a little higher than the expected value of (9.046±0.004) kJ mole^{-1} [38].

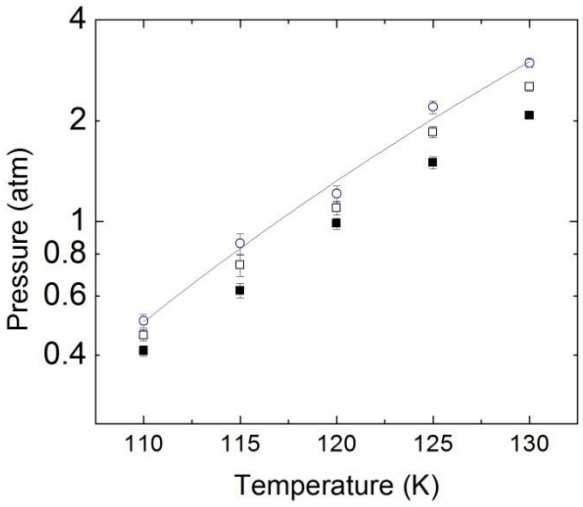

Fig. 2.3 Vapor pressure vs. temperature *T* for a 5 layer system consisting of a 50-50 mixture of Kr^{78} and Kr^{90}. The pressure was calculated at the 20% and 10% desorption times and extrapolated linearly to the 0% time (fill circles) via the expression $P_{vap}(0\%) = 2P_{vap}(10\%) - P_{vap}(20\%)$ .The solid line is a fitted Clausius-Clapeyron vapor pressure curve.

The melting temperature is determined by analyzing the potential energy versus temperature and by taking the midpoint at where the slope of the potential energy is the steepest. The implied krypton boiling point was determined to be 117±1 K compared to the experimental value of 199.93K [38]. To generate the data to determine the melting temperature, a monolayer of Krypton is adsorbed onto a sheet of graphite where the interaction potentials used are the same as those described in the previous sections. The system is equilibrated for 40 ps at a given temperature (ranging from 90 – 130) K, after

which the appropriate averages were calculated for another 100 ps at the same temperature.

Figure 2.4 shows the plot of the total adlayer potential vs. temperature.

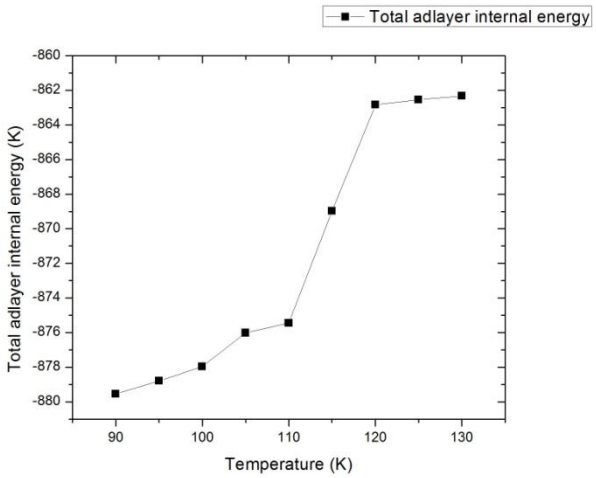

Figure 2.4 Total adlayer internal energy vs. temperature. The melting point can be determined by looking at the midpoint of where the total potential has the greatest slope.

The plot shows the potential has a sharp jump from T = 110 K to T = 120 K, which signifies that the melting temperature is T = 115 ± 5 K. When compared to the experimental value for the melting temperature of a monolayer of Krypton 115.9 K[38 39]. With the molecular dynamics simulation being able to approximate both the vapor pressure and the melting point of Krypton, we can assume proper use and choice of the interaction potential and algorithms as well as the validity of the code.

The subject of efficiency of a program is based more on preference. The program could be more efficient it the code was written for use on parallel processors or if the arrays used to keep track of how many particles have left were only the size that was needed. Since these changes would require more time to implement, the amount of time that would be saved was deemed to be negligible compared to just running the code as is. As is the total simulations ran in this work required 90 processors running for 12 weeks straight.

2.7e. Competency of Usage

The more complex the software, the easier it will be to make a mistake that results in false information. Even if the program used has a proper structure and the algorithms are coded correctly, it is still possible to use the wrong input parameters. The previous sections described the models used for the potential interactions, the algorithm that is used for updating the position, velocity and the acceleration as well as the condition for desorption. This was followed by validating the melting point of a monolayer of Krypton physisorbed onto graphite as well as the vapor pressure for a multi-layer Krypton structure physisorbed on graphite.

The only parameters left to discuss are the input parameters that were used for the Kr-Kr and Kr-graphite interactions. The values used were taken from previous theoretical work[40 41] that was done on similar configurations.

The parameters used are listed in Table 1 below.

Quantity	Symbol	Value
Kr-Kr potential parameters	$\varepsilon_{Kr}, \sigma_{Kr}$	171.0 K , 3.6 Å
Kr-graphite potential parameters	$\varepsilon_{Kr-C}, \sigma_{Kr-C}$	64.83 K, 3.22 Å
Graphite plane spacing	D	3.37 Å
Area of graphite unit cell	a_s	5.24 Å
Atom number in unit cell	Q	2

Table 1 Input parameters for LJ and Steele interactions

Chapter 3 Results of Molecular Dynamics Desorption Model

To investigate the behavior of the krypton isotopes as they desorb from graphite, Fig. 3.1a is a plot of the number of lighter isotopes, N_L, and the number of heavier isotopes, N_H, as a function of time. Two different configurations were initially used: the first was a monolayer of krypton isotopes on graphite, while the second was of a 5 layer system of krypton isotopes adsorbed onto graphite. Both configurations consisted of a 50% mixture of Kr^{78} for the lighter mass and Kr^{100} for the heavier mass, with the system temperature was kept constant at T = 120K.

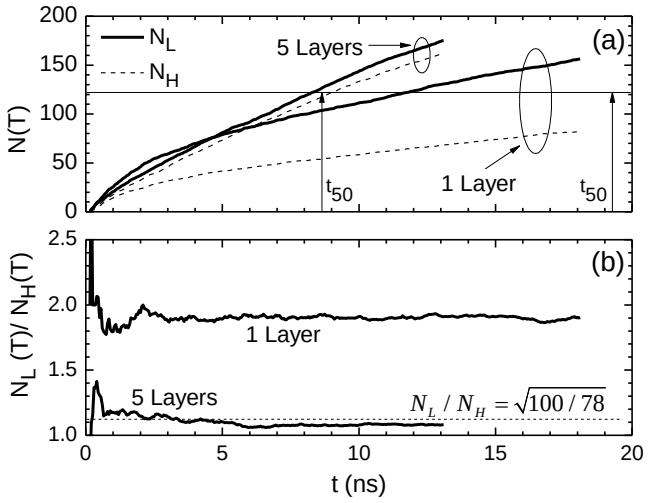

Fig. 3.1 (a) Number of light (N_L, Kr^{78}) and heavy (N_H, Kr^{100}) isotopes that have desorbed from the surface as a function of time for 1 and 5 adsorbed layers at 120K. (b) Ratio of desorbed isotopes N_L/N_H vs. time.

The 5 layer system seen in Fig3.1a has a nearly constant rate of desorption which might suggest the desorption rate is following zero order kinetics, associated with a rate of desorption that is independent of the coverage [42]. The rate of desorption for the 1 layer system is initially higher until the approximately 20% of the isotopes desorb from the system, at which point the rate is approximately half of the 5 layer system. The change in the desorption rate for the 1 layer system might be due to the possibility of the formation of islands or clusters which would have a significant influence on the desorption rates [43].

Figure 1b is a plot of the ratio of N_L/N_H as a function of time. After the initial fluctuations seen in the ratios, which are due to the small number of isotopes that have desorbed from the system, the ratio stabilizes near a constant value. Even though it will be discussed later, it is worth noting that the ratio in the 5 layer system stabilizes near the value that one would expect if the system were to follow Graham's law, $\sqrt{100/78}$ = 1.13. In comparison, the one layer system exhibits a constant value that is significantly higher, 1.9 than would be expected if Graham's law was expected to be followed.

Since the ratio of the isotopes that have desorbed from the system is approximately independent of time, we identify the time t_{50} at which 50% of the isotopes in the system have desorbed and define the isotope separation effect, S_{50} as the ratio

$$S_{50} = N_L(t_{50}) / N_H(t_{50})$$

where $N_L(t_{50})$ and $N_H(t_{50})$ are the number of lighter and heavier isotopes that have desorbed by time t_{50}.

To determine if there is a temperature dependence on S_{50}, simulations of krypton isotope pairs Kr^{78}/Kr^{90} and Kr^{78}/Kr^{120} were initialized with 5 layers and S_{50} was calculated over the temperature range 110-130K. Fig. 3.2 is a plot of S_{50} vs. temperature where each data point represents mean value and the standard error for 10 simulations. The data is fit to a straight line to establish if there is a trend in S_{50} over the temperature range being investigated. The data shows that over the temperature range T =110K to 130K there is no significant temperature dependence and we conclude that it is sufficient to evaluate S_{50} at one temperature.

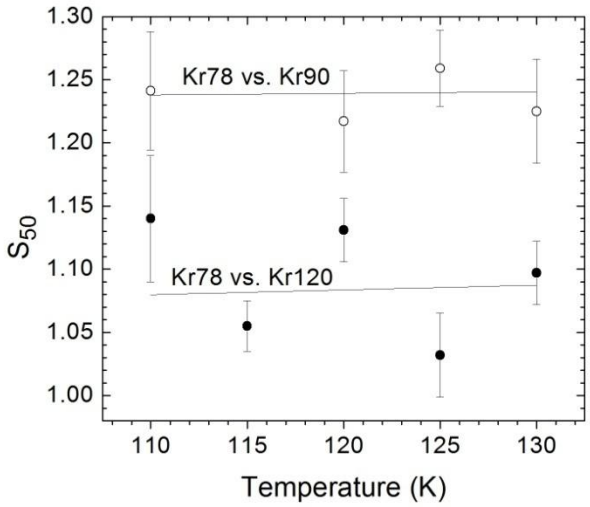

Fig. 3.2 S_{50} vs. T for mixtures of Kr^{78}/Kr^{90} and Kr^{78}/Kr^{120} for a 5 layer system.

To investigate the effect the graphite substrate has on the desorption rate of the isotopes, Fig. 3.3 is a plot of S_{50} as a function of the number of initial adsorbed layers for the isotope pair Kr^{78}/Kr^{100} where each data point is the mean and standard error from 10 simulations. As suggested from the previous graph, as the number of initial adsorbed layers decreases, S_{50} increases. To test whether the effect seen is due to the large mass separation used, 62 simulations were also run for a monolayer system of Kr^{78} and Kr^{86} as well as 20 simulations for a bi-layer system with the same mass. As the data in Fig. 3.3 shows, the large separation effect seen for small layer thicknesses is not simply due to the large mass separation.

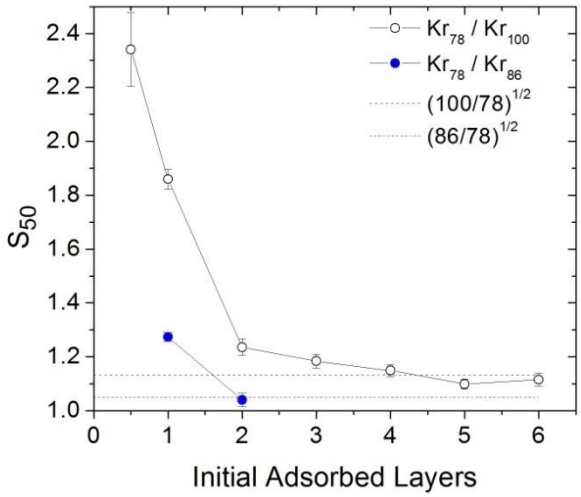

Fig. 3.3 S_{50} vs. number of initial adsorbed layers for Kr^{78}/Kr^{100} and Kr^{78}/Kr^{86} mass pairs at T=120K.

The effect the graphite substrate has on the desorption of the isotopes can be further seen by looking at the time it takes, t_{50} for half the isotopes to desorb from the system as a function of initial adsorbed layers, Fig. 3.4.

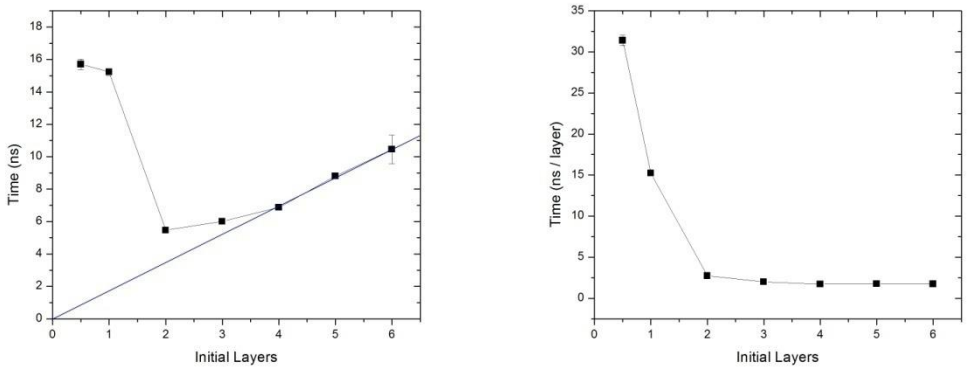

Fig. 3.4. a) t_{50} vs. initial adsorbed layers for Kr^{78} and Kr^{100}
b) t_{50}/initial number of layers vs. number of initial adsorbed layers.

Looking at the trend from Fig. 3.4 and comparing it to the trend seen in Fig 3.3, suggests that the graphite plays a significant role in the confinement of the monolayer, by restricting the desorption process to only those isotopes which have the greatest energy. The fact that the time for half of the isotopes to desorb from the system increases past the second layer is most likely due to the fact that the isotopes have a greater restriction on their movement due to the potential interaction between the increasing number of nearest neighbors.

To further compare the multilayer system and the monolayer system, S_{50} is compared to the mass ratio in Fig. 3.5. Taking as a model that S_{50} is proportional to the effective mean rates of desorption for each pair of masses, the data has been fit to a Graham's law like expression,

$$S_{50} = (M_H / M_L)^{\gamma}$$

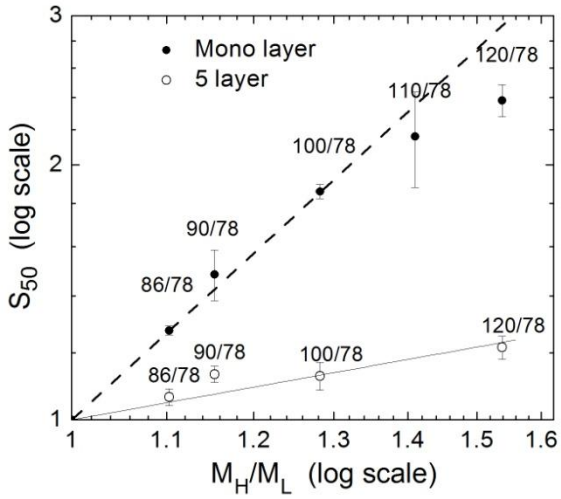

Fig. 3.5 Ratio of the mean desorption rates for both monolayer and 5 layer systems at T = 120K.

The fitted lines yield γ=2.8±0.14 and γ=0.49±0.14 for the 1 layer and 5 layer system respectively. The monolayer calculations from 86 amu to 120 amu used, respectively, 62, 8, 19, 9 and 27 simulations of 484, 100,484, 100 and 100 particles each. For the 5 layer system, γ=0.5 which is in agreement with Graham's law, suggesting that migration of the krypton atoms between layers is cancelling the lack of isotope effect that would be associated with strict layer by layer desorption. The larger mass ratios seen in the monolayer case isn't included in the fit due to the fact that it does not agree with the closer mass separations.

To look at the effect seen in the previous plot in more detail, a snapshot at t = 1 ns of the molecules' positions along the z-axis was acquired from one of the simulations of a 5 layer system of Kr^{78} and Kr^{100} on graphite at a temperature of T=120K. After 1 ns, it can

be seen that roughly half of the atoms initially in the second layer have left their parent layer. The evident lack of migration seen in the histogram for the first layer is most likely due to the enhanced confinement provided by the strong attractive potential of the graphite substrate[44]. The trend in Fig 3.6 further supports the data previously shown that the graphite substrate has little to no effect on the desorption rate of the upper layers as seen by the significant mixing of the layers after 1 ns.

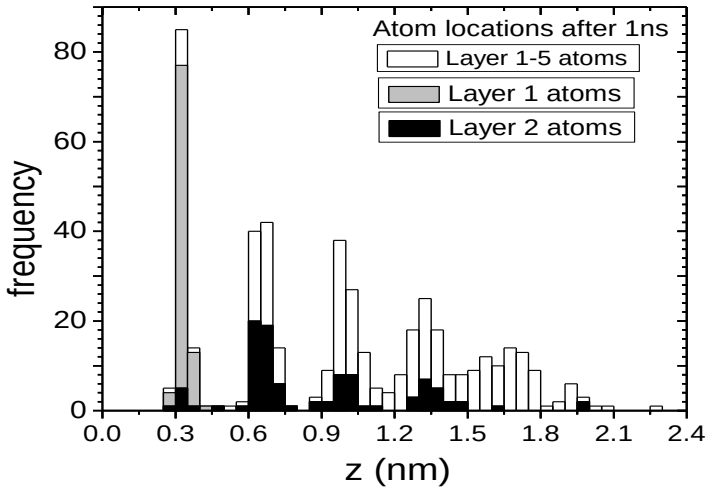

Fig. 3.6 Distribution of 500 atoms of Kr^{78} and Kr^{100} in a 5 layer system at T=120K vs. vertical distance from the graphite substrate, after 1 ns.

Chapter 4 Results and Discussion

We have considered a Molecular Dynamics computer simulation of multi-layered krypton isotopes physisorbed onto a graphite surface. The particle-particle interactions were modeled through the use of a standard 12-6 Lennard Jones potential and the particle substrate interaction was modeled through a modified Lennard Jones potential proposed by Steele. By keeping the adsorbed atoms at the same temperature through velocity rescaling and removing isotopes from the potential and temperature calculations when they desorb from the system, we were able to look at the rates of desorption as a function of mass as well as a function of physisorbed layers and temperature. It has been shown that while keeping the system temperature constant in a binary mixture of krypton isotopes, the ratio of the rates of desorption is in agreement with Graham's Law for multilayered systems. Analysis of the isotope separation as a function of temperature shows little to no change over the temperature range T = 110 – 130 K. This is believed to be a result of the upper layers melting and having more mobility than the layers of isotopes beneath it. While the lower layers are less mobile than the layers above, we show that inter-layer diffusion of the isotopes is possible for adsorbed layers past the first layer. This statement can be further validated by the fact that each layer had approximately a 50-50 mixture of the Krypton isotopes. If an isotope effect was seen, it would imply that the atoms from under the highest layer (with respect to the perpendicular distance from the graphite) would be moving through diffusion to the surface of the Krypton system.

When the isotope effect was analyzed as a function of layer, it was discovered that monolayer systems exhibited a pronounced effect on the rates of desorption of the isotopes. While the multi-layered systems (adsorbed layers > 2), desorbed at a relationship approximately equal to Graham's Law, $(m_H / m_L)^{1/2}$, the monolayer system desorbed at a rate that closer to $(m_H / m_L)^2$, where m_L and m_H are the light and heavy isotopes in a binary mixture.

While our results suggest a significant improvement in isotope separation in using only monolayer systems, there are several components of our model that could be improved upon, not only to validate the results further, but to make the model more realistic. These components fall into one of three areas: particle-particle/particle-substrate interactions, temperature control and the choice of the desorption point.

While using a Lennard Jones potential to model the interaction between particles in Molecular Dynamics is standard, it is well known that there are potentials that would recreate a more realistic interaction. The LJ potential was used in our case, due to the low computational cost and the ease of implementation. The interaction between the graphite and the Krypton isotopes is modeled through a truncated Fourier expanded LJ potential. The interaction potential was chosen due to its ability to offer a tremendous savings in terms of computation time. Several computational studies using this interaction potential

have shown the reliability and accuracy of this interaction potential when comparing the results to those found through experimental methods[45 46 47 48 49].

While the model designed does not explicitly include the sticking coefficient between the Krypton adatoms and the graphite substrate, it is implicitly included due to the use of the velocity rescaling method. This can be seen by imagining how the kinetic energy of a single atom would change as it is shot at the bare graphite surface modeled in our simulation. As the atom approaches the graphite surface, it is speed up due to the large attractive force between the particle and the graphite. At each timestep, the particle's velocity is checked and compared to its expected value using the equipartition theorem. If the particle has a greater kinetic energy than it should for a given temperature, it is slowed and depending on the angle of incidence, it could stick to the surface. In a system of N atoms, this would cause for a sticking of the incident atoms on the substrate even though it isn't explicitly included in the design.

An approximation of the sticking coefficient in the model could be calculated by determining the vapor pressure for both a Krypton monolayer system adsorbed on graphite and a 5 layer Krypton adsorbed on graphite. By equating the number of particles hitting a surface to the number of particles leaving, through the use of the Polanyi-Wigner equation and the ideal gas law, the pressure can be written as

$$P \cdot S(\theta,T) = \frac{4 \cdot k \cdot T}{\bar{v}} \cdot \nu(\theta,T) \cdot \theta^1 \cdot e^{\left(\frac{-E_d(\theta,T)}{kT}\right)}$$

where $S(\theta,T)$ is the sticking coefficient. To calculate the other terms in the Polanyi-Wigner equation one could use an Arrhenius type plot:

$$\ln(k) = \ln(A) - \frac{E_d}{R}(\frac{1}{T})$$

By plotting the log of the rate (k), versus the inverse temperature for several different temperatures the attempt frequency (A) and desorption energy (E_d) for each species could be determined. Then by taking the ratio of the pressures for a monolayer system and that of a multilayer system the sticking coefficient could be determined.

The sticking coefficient is difficult to determine not only because of the model being used but as in the fact that it changes as a function of coverage. Sub-monolayer experiments and simulations[50 51] have shown the formation of islands on substrates. Since the sticking coefficient is dependent upon coverage, the formation of islands, and their size, further investigations need to be done on the influence of using interaction potentials on the sticking coefficient.

The temperature control method implemented is of the most basic kind and serves as a very rough method to keep the system temperature constant. Work done by Hermansson and Clementi showed how even with small time steps, the use of velocity rescaling in Molecular Dynamics to keep the system at a constant total energy can have drastic effects on the trajectory and velocity of the particles involved[52]. While the effects of velocity rescaling on the trajectory and velocity of the particles involved cannot be ignored, we

are still confident in our results due to the fact that several simulations were performed ($n \geq 10$ for all multilayered simulations, $n \geq 20$ for simulations based on layers and $n = 62$ for the Kr_{78} and Kr_{86} monolayer simulation), that would have wash out any statistical abnormalities. While we are confident in our model design, it does not mean that it cannot be improved, by using a better thermostat such as the Nose Hoover or Berendsen thermostat that allows for the temperature to be changed in a more realistic manor.

Lastly, the other parameter that needs to be investigated to determine its significance in our results is the desorption point for the isotopes. In our simulation we defined the point of desorption to be a value on the z-axis that is approximately 3σ above the highest layer in adsorbed Krypton system after equilibrium. While the LJ potential is usually truncated in most Molecular Dynamics at this point, doing so when depending upon the dynamics of a system may have negative consequences. At distances of approximately 10 angstroms, isotopes that are nearing the point of desorption would feel a greater attraction on them. This would decrease the overall rate of desorption but it would do so equally over all the isotopes. Therefore, extending the range at which the isotopes have left the system would simply extend the length of the simulation.

Even with the use of a simple model we have demonstrated that there could be a definite advantage to separating isotopes using physisorbed systems. Further improvements could be made considering that our simulation only modeled physical adsorption. Physical adsorption is due to a relatively weak Van der Waal attractive force and takes place on all

surfaces considering that the temperature and pressure conditions permit. Another form of adsorption that could be considered is chemical adsorption. Chemical adsorption only takes place as long as the adsorbed particle can make contact with the surface. Since chemical adsorption is a single layer process and provides a stronger confinement than physisorbed particles, it may prove to be much more effective in isotope separation. While our research was centered on the idea of isotope separation, it may also prove useful to any system where the particles/molecules involved need to be separated. By using a combination of both physisorption and chemisorptions systems could be designed to take advantage of the interaction between substrate and adsorbate to facilitate a more favorable separation than those currently available.

[1] Soddy, Fredrick, Nature (1931) 399-400

[2] www.atomicheritage.org/index.php/component/content/172.html?task=view

[3] Mason, E. A. , Kronstadt, Barbara, Journal of Chemical Education (1967) 740

[4] Beams, J. W., Haynes, F. B., Physical Review, **50** (1936) 491-492

[5] NIEMANTSVERDRIET, A.M. et al, Surface Science **41** (1990) 232.233

[6]Redondo, A. , et al. Phys. Rev. Letters, **49** (1982) 1847-1850

[7] Asada, Hiromu , Masua, Makihiko, Surface Science **207** (1989) 517-524

[8] Kreuzer, H.J. , Payne, S.H. Studies in Surface Science and Catalysis **104** (1997) 153-200

[9] Payne S. H.and Kreuzer H. J. , Surf. Sci. **338**, (1995) 261-278

[10] Asada H, Sekito H, Surface Sci. **273** (1992) 139-146

[11] Allen MP and Tildseley, DJ, *Comp. Sim. of Liquids* , New York: Oxford , 1987

[12]W.G. Wyckoff , *Cry. Structures*. New York, London: John Wiley & Sons, 1963

[13] Steele, W.A. , Surf. Sci. **36** (1973) 317

[14] WA Steel. Gas-Solid Interface. New York: Marcel Dekker, 1964 Vol. 1.

[15] A Clark. Theory of Adsorption and Catalysis. New York: Academic Press,1970

[16] Toth, Jozsef, ed. *Adosorption Theory, Modeling and Analysis*. New York: Marcel Dekker, 2002. Print.

[17] Stone, A.J. Science **321** (2008) 787-789

[18] Metropolis, N et al. Chem. Physics , **21** (1953) 1087-1092

[19] Youn, H.S. , Meng, X.F. and Hess, G.B. Phys. Rev. B **48** (1993) 14556 - 14576

[20] Migone, A. D. et al , Phy. Rev. Letters **51** (1983) 192 -195

[21] Koch, S.W. , Rudge, W. E. and Abraham, F.F **145** (1984)

[22] Houlrik J M and Landau D P Phys Rev. E **50** (1994) 2007-2013

[23] F. F. Abraham, Adv. Phys. 35, 1 (1986

[24] J. E. Lane and T. H. Spurling, Aust. J. Chem. **29** (1976) 2103

[25] F. Hanson and J. P. McTague, J. Chem. Phys. **72** (1980) 6363

[26] F. F. Abraham, S. W. Koch, and W. E. Rudge, Phys. Rev. Lett. **49** (1982) 1830

[27] Houlrik, J.M., et al,Phys. Rev. E **50** (1994) 2007

Khokonov, A.et al, B.S., Surf. Sci. Lett. **496** (2002) 13

[29] Andersen, Hans C. (November 2001) "Accuracy of Integrators for Equations of Motion in Molecular Dynamics" *Lecture Notes, Chemistry 276.* Stanford University. ONLINE: http://chemweb.stanford.edu/fall2001/chem276/c276_01_lecture11.pdf

[30] Fan, Jinghong. *Multiscale Analysis of Deformation and Failure of Materials*. UK: John Wiley and Sons Ltd. 2011

[31] Ciccotti, G.; Hoover, W. G. MD Simulation of Statistical-Mechanical Systems; North-Holland:Amsterdam, 1986.

[32] Choe, Jong-In and Kim,Byungchul. Bull Korean Chem. Soc. **21** (2000) 419-424

[33] Berens, P.H, Mackay, D. H. et al, K.R. **79** (1983) 2375 - 2389

[34] Lantelme F, Mol. Phy. , 47 (1982) 1277-1284

[35] Gunsteren W and Mark A, J. Chem. Phy. , **108** (1998) 6109-6116

[36] Butler D.M et al, Phy. Rev. Lett. **42** (1979) 1289

[37] Horn PM , Birgeneau, R J, et al, Phy. Rev. Lett. **41** (1978) 961

[38] Ferreira A G M , Lobo L Q , J of Chem Thermodynamics **41** (2009) 809-815

[39] Kemp R C and Kemp W R G, Metrologia **14** (1978) 83

[40] Bader K and Roth M W, Surface Sci. **538** (2003) 30-44

[41] S. W. Koch, F. F. Abraham, and W. E. Rudge, Surface Sci. **49** (1984) 329

[42] H. Ulbrict, R. Zacharia, N. Cindir and T. Herte, Carbon **44** (2006) 2931-2942

[43] M. Bowker, Surf. Sci. **100** (1980) L472-L474

[44] A. Mulero and F. Cuadros, eds. Adsorption Theory, Modeling and Analysis. (New Yrok: Marcel Dekker Inc, 2002) p.160 Print

[45] SteeleWA, Surface Sci. **36** (1973) , 317

[46] Monson PA, Steele WA , Henderson D, J Chem Phys **74** (1981) 6431

[47] Monson PA , Cole MW, Toigo F , Steele WA , Sur Sci **122** (1982) 401

[48] Siddon RL, Schick M, Phys Rev A **9** (1976) 2501

[49] Sander LM , Bretz M , Cole MW, Phys Rev B **14** (1976) 61

[50] Kreuzer H J, Sur. Sci. **344** (1995) 1264-1270

[51] Friess W, et al. , Sur. Sci. Let. **298** (1993) 173-180

[52] Hermansson,Kersti,Lie, George and Clementi,Enrico, J. Comp. Chemisty **9** (1988) 200-203